

Regional climate simulations for the Barents Sea region

Elke Keup-Thiel, Holger Göttel and Daniela Jacob

Max Planck Institute for Meteorology, Bundesstraße 53, D-20146 Hamburg, Germany

Received 15 June 2005, accepted 2 Mar. 2006 (Editor in charge of this article: Veli-Matti Kerminen)

Keup-Thiel, E., Göttel, H. & Jacob, D. 2006: Regional climate simulations for the Barents Sea region. *Boreal Env. Res.* 11: 329–339.

The vulnerability of the Barents Sea region to climate change is under investigation in the context of the EU Project BALANCE (<http://balance1.uni-muenster.de>). Today's climate of the Barents Sea region has been simulated using the regional climate model REMO driven by Analysis (since 1994) and by Reanalysis (1979–1993) of the European Centre for Medium-Range Weather Forecasts (ECMWF) from 1979 to 2000 with a horizontal resolution of about 55 km. The results have been validated using observations from the Climatic Research Unit (CRU data) for 2-m temperature and precipitation for land areas only. The differences between the REMO simulation results and the CRU data are of the same order of magnitude as the deviations between CRU data and ERA-40 data (Reanalysis data of the European Center for Medium-Range Weather Forecasts). To investigate a possible future climate development a 140-year-long transient simulation from 1961 to 2100 has been carried out using REMO. In this experiment, called the CCC run (Control and Climate Change run), REMO has been driven by ECHAM4/OPYC3 following the IPCC-SRES B2 scenario. The annual mean 2-m temperature of the CCC run shows a clear trend as expected, the 2-m temperature increases by 5 °C by the end of the century. The Arctic Climate Impact Assessment reports a 1.5 °C temperature increase from 1960 to today, which is in good agreement with our results. From 1960 to 2000 the observed annual mean temperature for the Arctic rises exactly in the same way as in the REMO simulation for the Barents Sea only. Three 20-year periods have been defined in order to analyze differences among these time slices. A stronger warming in January than in July is evident for all time slices. As expected, the warming is enhanced for the period 2041–2060 as compared with that for the earlier period (2011–2030). The largest warming occurs along the sea ice edge and over Russia during the winter months.

Introduction

The Arctic climate is of special importance. The sensitivity of this region to climate change has given the motivation to conduct several studies and international projects: The Arctic Climate Impact Assessment (ACIA, 2004: Impacts of a warming arctic, <http://amap.no/acia>), the Arctic Ocean Model Intercomparison Project (AOMIP,

http://fish.cims.nyu.edu/project_aomip/overview.html) and the Arctic Regional Climate Model Intercomparison Project (ARCMIP, <http://curry.eas.gatech.edu/ARCMIP/index.html>). The variability of temperature and precipitation in the entire Arctic region has been documented and a summary of available measurement stations and historical schedules has been given by Przybylak (2002). Regional modeling studies

were performed for example by Lynch *et al.* (1995, 2001, 2004) and Dethloff *et al.* (1996, 2001). The importance of the Arctic climate for the European weather conditions (Semmler 2002) and the changes of the Arctic climate in response to scenarios prepared by the Intergovernmental Panel on Climate Change (IPCC) were investigated for example with the regional model REMO by Pfeifer and Jacob 2005. Their study points out whether the presented scenario calculation indicates an anthropogenic climate change or not. In their study, they analyzed global climate scenario calculations with the global climate model ECHAM4 (Roeckner *et al.* 1999) to demonstrate the internal variability of the Arctic climate. In addition, they conducted REMO simulations for the period 2070 to 2079 to assess the smaller scales of the Arctic climate change. They conclude that the regional climate model simulates quantitatively the same changes as the global climate model does, but its advantages are clearly related to the high amount of detail, which becomes obvious when looking at the spatial pattern of the signal.

In the Special Report on Emission Scenarios (SRES, Nakićenović *et al.* 2000, Houghton *et al.* 2001) atmospheric conditions have been defined to appoint conceived scenarios. For example, the B2 scenario describes a world orientated towards environmental protection and social equity with emphasis on local solutions to economic, social and environmental sustainability. In the B2 scenario a moderate CO₂-increase and SO₂ decrease are assumed. The CO₂ emissions assumed for the B2 scenario lie in the middle of the other IPCC scenarios. For the A1B scenario a greater CO₂ emission increase is assumed until 2050 and a decrease afterwards. For the B1 scenario the assumed CO₂ emission is clearly less than the CO₂ emission of the B2 scenario. The B2 scenario has been chosen together with our EU-project partners for our investigation with the regional climate model REMO.

The vulnerability of the Barents Sea region to climate change is investigated in the context of the EU-Project BALANCE (<http://balance1.uni-muenster.de>). In co-operation with fifteen participating institutes from Norway, Sweden, the Netherlands, Finland, the United Kingdom and Germany, the influence of climate change

on the Barents Sea region is studied. This project addresses a large variety of components, including the terrestrial and the marine ecosystems as well as some of the economic sectors, such as fishery, forestry and reindeer husbandry. Climate change is affecting living conditions for humans, vegetation and animals in the Arctic. The basis for these advanced studies in BALANCE is the Control and Climate Change run (CCC-run) performed with the regional model REMO. The goal of the study presented here, is to highlight possible future changes of temperature, precipitation and snowfields in the Barents Sea region, with a higher spatial resolution than offered by global climate models.

After a short model description and a specification of the experimental setup, a validation of the baseline run using the Climate Research Unit data set, called the CRU data (New *et al.* 2002), and reanalysis data of the European Center for Medium Range Weather Forecasts (ERA-40) is presented. This part of the paper indicates the quality of the regional model results for the region under investigation and serves as trust building for the climate change analyses. The major part of the paper is related to the analysis of the climate changes in temperature and precipitation fields in the Barents Sea region, utilizing time series and differences of 20-year means of these quantities.

Model description and experimental setup

REMO is a regional hydrostatic climate model and is used in different regions all over the world depending on available boundary conditions. It has been developed at the Max Planck Institute for Meteorology (MPIfM) (Jacob and Podzun 1997, Jacob 2001, Jacob *et al.* 2001) as the atmospheric component of a coupled atmosphere-hydrology model system. Applications of REMO have included the simulation of the energy and water cycle over Europe within the international BALtic Sea EXperiment (BALTEX) (Raschke *et al.* 1998, 2001). REMO was also involved in the evaluation of an ensemble of eight different regional climate models over the Arctic Ocean (Rinke *et al.* 2006)

and additionally in the intercomparison of six regional climate models in modeling the Arctic boundary layer (Tjernström *et al.* 2005).

For simulations of today's climate of the Barents Sea region REMO has been driven by Analysis/Reanalysis of the European Center for Medium-Range Weather Forecasts (ECMWF). The integration of REMO from 1979 to 2000 is called the baseline run. This baseline run has been used for comparisons with observations.

To investigate possible future climate development, REMO has been driven by the transient ECHAM4/OPYC3 IPCC-SRES B2 scenario. This run is called Control and Climate Change run (CCC run) and has been performed to simulate the climatic change of the Barents Sea region from 1961 to 2100. The ECHAM4/OPYC simulation started 1860 with SST values close to those of 1990 and has therefore a warm bias in the sea surface temperature (SST). It was suggested by Roeckner *et al.* (1999) to analyze only differences of time slices and not the absolute values themselves.

The simulation domain is shown in Fig. 1. All simulations have been conducted with 1/2° horizontal resolution in a rotated grid.

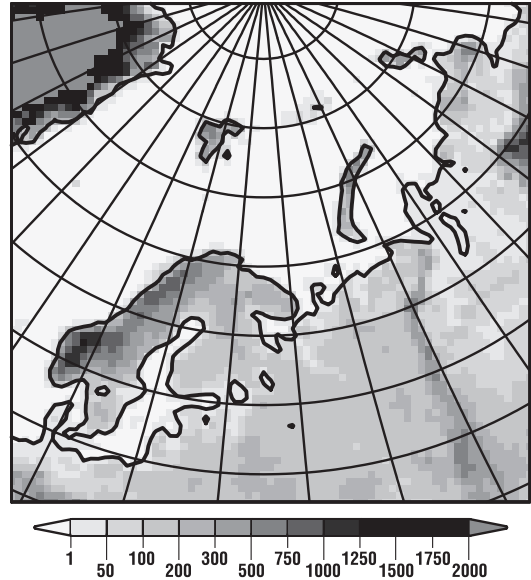


Fig. 1. Simulation domain of the Barents Sea region with model orography (m).

ECMWF Reanalysis data (ERA-40). A direct comparison of temperature data for Norway, Finland and Sweden has been carried out because other Arctic areas especially Russia have bad data coverage (Fig. 2). The comparison of the annual cycle between simulated and observed data reveals warmer simulated winter months (about 2 °C) and colder simulated spring and early summer months (about 1 °C) for Norway and Sweden. For Finland the 2-m temperature during April shows the strongest deviation (Fig. 3). The differences between the baseline run and CRU data are of the same order of magnitude as the deviations between CRU and ERA-40. In

Validation

Results of the baseline run in the period 1979 until 2000 have been validated with observations using a high resolution data set of surface climate over land areas from the Climate Research Unit (New *et al.* 2002) and against the

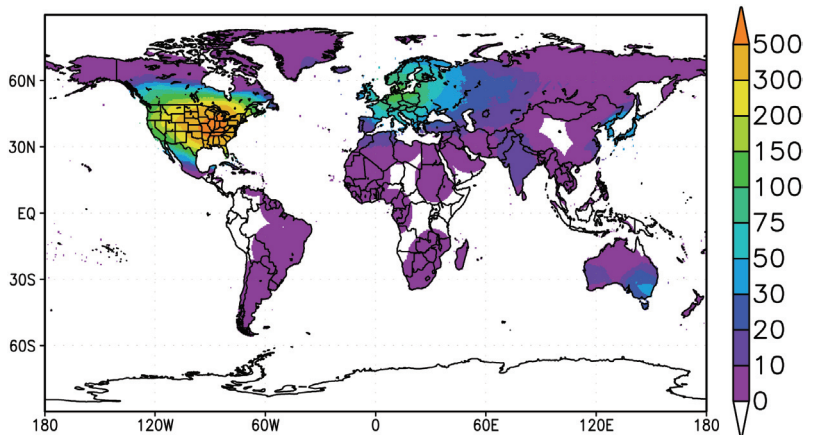


Fig. 2. Global distribution of available measurement data in the CRU data set. Shown here is the number of stations per grid area of CRU.

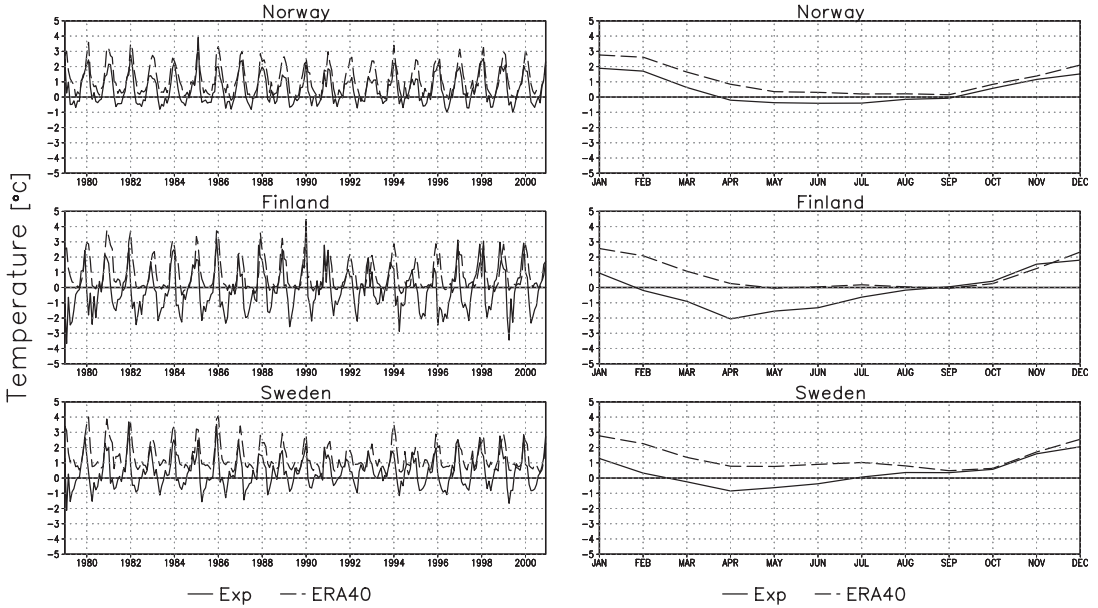


Fig. 3. Comparison of 2-m temperature (°C) between the ERA-40 data, REMO baseline run and CRU data set as a mean over Norway, Finland and Sweden. The left-hand side panel shows the time series and the right-hand side panel shows the mean annual cycles of REMO data and ERA-40 data in deviation to the CRU data set for Norway, Finland and Sweden.

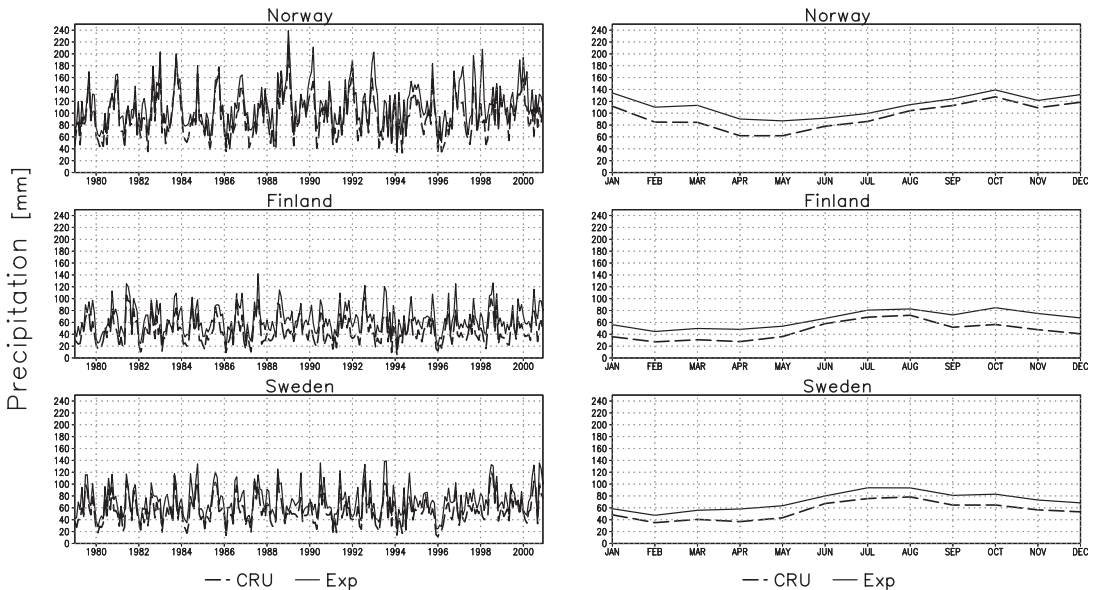


Fig. 4. Comparison of the precipitation rates (mm month^{-1}) from CRU data set (dashed line) and REMO (solid line) from 1979 until 2000 on the left-hand side. The mean annual cycles of precipitation rates of the baseline run of REMO (solid line) compared with the CRU data set (dashed line) on the right-hand side.

Finland, where the differences are strongest, the observation density is coarser than in Sweden or Norway (Fig. 2). This could be the reason for the relatively strong deviation between simulation and observation in Finland. The validation of

the precipitation data was executed for the same areas as shown in Fig. 4. The variability in the simulated precipitation is similar to the measured one (left-hand side of Fig. 4). The systematic overestimation of the precipitation in REMO

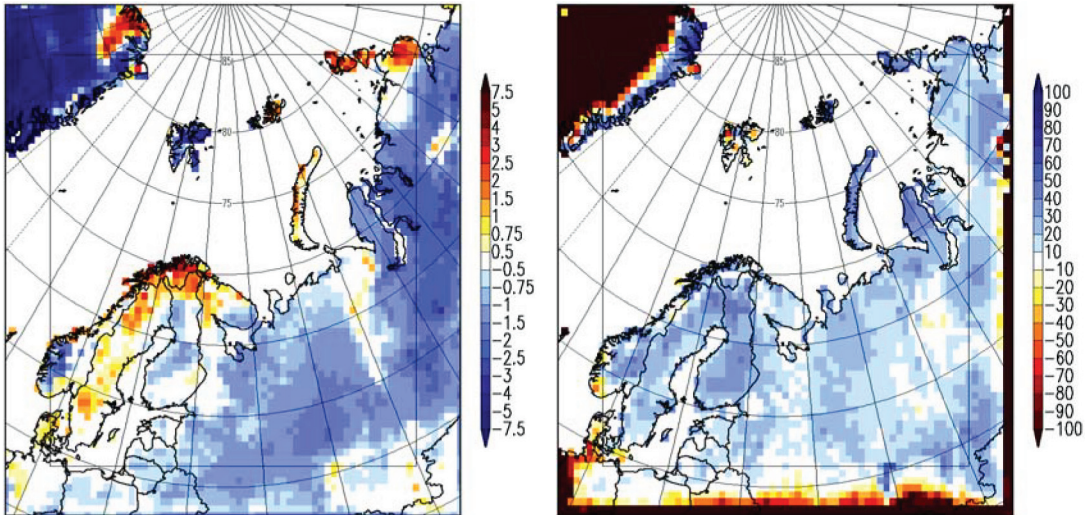


Fig. 5. Differences (Baseline – CRU) of the 2-m temperature ($^{\circ}\text{C}$) on the left-hand side and the relative difference of precipitation (%) on the right-hand side for the annual mean of the time slice (1981–2000).

(right-hand side of Fig. 4) is in the range of the measurement accuracy (B. Rudolf & F. Rubel unpubl. data).

The horizontal distribution of the difference between the bi-decadal annual mean 2-m temperature (1981–2000) of the baseline run and the CRU data set shows a warm deviation for Norway and Sweden (Fig. 5). The largest bias is located in the northern part of Norway. Over Russia REMO is systematically colder than the CRU data set. Under consideration of the coarse data coverage of the CRU data in Russia, the comparison of REMO and CRU data is very imprecise for that region. The same is true for the relative differences of the precipitation, but REMO seems to be about 20%–30% too wet over Scandinavia. The difference might be explained at least partly by a negative bias in the CRU data set that is based on uncorrected gauge measurements. This feature needs to be addressed in more detail, since an overestimation of precipitation in the simulation could lead to an overestimation of runoff calculated by the BALANCE partners.

Climate change scenarios for the Barents Sea region

The climate of the Barents Sea region has been simulated from 1961 until 2100 with REMO.

This Control and Climate Change run (CCC run) has been performed to study the future climate of the Barents Sea. The analysis of the scenario describes the hypothetical changes in the Barents Sea region in the next century according to the IPCC/SRES B2 scenario (Houghton *et al.* 2001). In the B2 scenario a continuous CO_2 increase weaker than in the A1B scenario and a SO_2 decrease is assumed. As a first result, annual mean time series of temperature and precipitation will be presented. Additionally, time slices of 20-year periods have been investigated to figure out in which season and in which region the largest changes in temperature and precipitation are located.

As expected, the annual and area mean 2-m temperature of the CCC run in the Barents Sea region shows a clear trend, the 2-m-temperature increases by 5°C in 140 years (Fig. 6). The area mean is calculated over the model domain shown in Fig. 1. The mean temperature over land is generally higher than the mean temperature over sea (not shown). The Arctic in the Arctic Climate Impact Assessment report (ACIA, 2004: Impacts of a warming arctic, <http://amap.no/acia>) notifies a 1.5°C increase from 1960 to today, which is in good agreement with our results. From 1960 to 2000 the observed annual mean temperature of the Barents Sea region rose exactly in the same way as in the simulation.

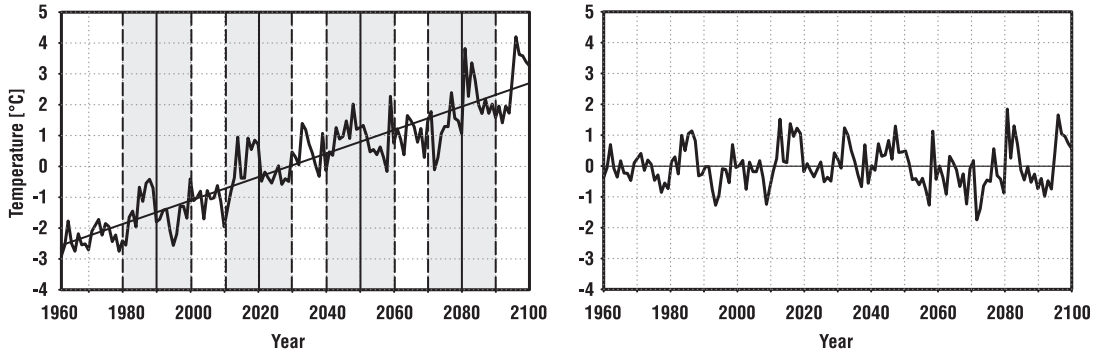


Fig. 6. Annual mean 2-m temperature ($^{\circ}\text{C}$) rise in the CCC-run for 1960–2100 on the left-hand side. The black vertical lines mark the time slices. A 20-year mean around these time slices (gray marked) is analyzed separately. On the right-hand side the annual 2-m temperature variability for the detrended time series is shown.

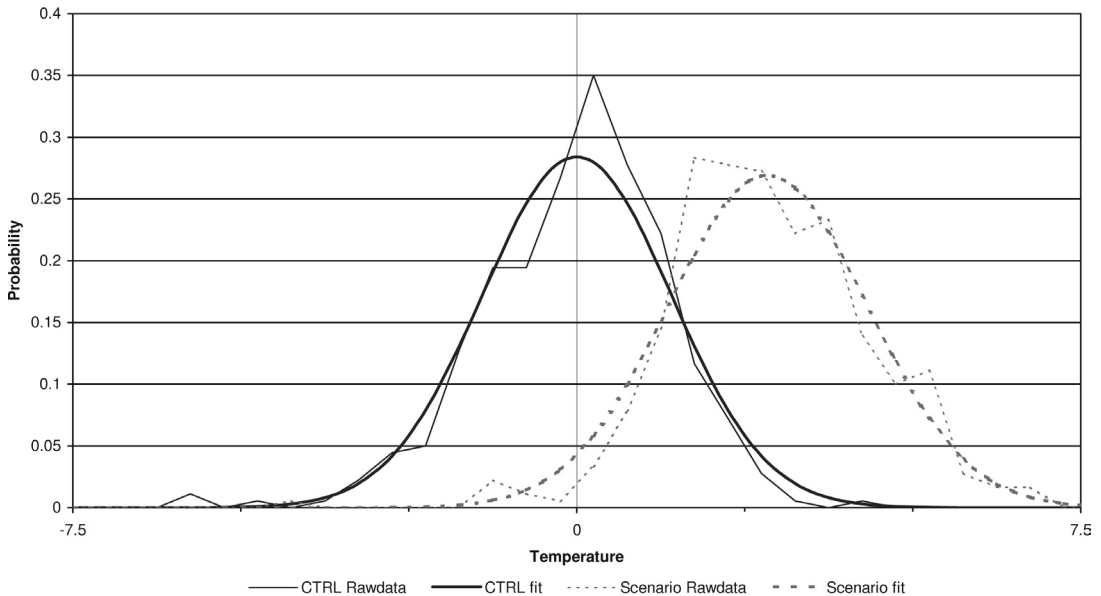


Fig. 7. Results from the regional climate change simulation representing today's (CTRL: 1961–1990) and future (scenario: 2061–2090) scenario conditions. Statistical distributions (without trend) of monthly temperature anomalies for Norway (with respect to the reference period 1961–1990) for today and for the scenario. The bold line shows the fit with the Gaussian distribution, thin lines are obtained from raw data with an interval of 0.5°C .

To demonstrate the inter-annual variability of the 2-m temperature, the detrended time series (Fig. 6, right-hand side panel) and the frequency distribution of Norway monthly temperature anomalies to the reference period 1961–1990 (Fig. 7) are shown. A clear shift of the frequency distribution by $\sim 2.8^{\circ}\text{C}$ towards warmer temperatures can be seen in 2061–2090. The distribution for the future period is also slightly wider, but the increase in variability is not statistically significant.

The time series of the annual mean precipitation rate for the whole model region shows an increase in precipitation from 58 to 74 mm month $^{-1}$ from 1960 to 2100 (Fig. 8, left panel). The annual mean precipitation over land is generally higher than over sea (not shown), both time series show a clear trend for the whole period. The annual precipitation rate varies around 15–20 mm month $^{-1}$ (Fig. 8, right-hand side panel). No change in precipitation variability can be detected from this curve.

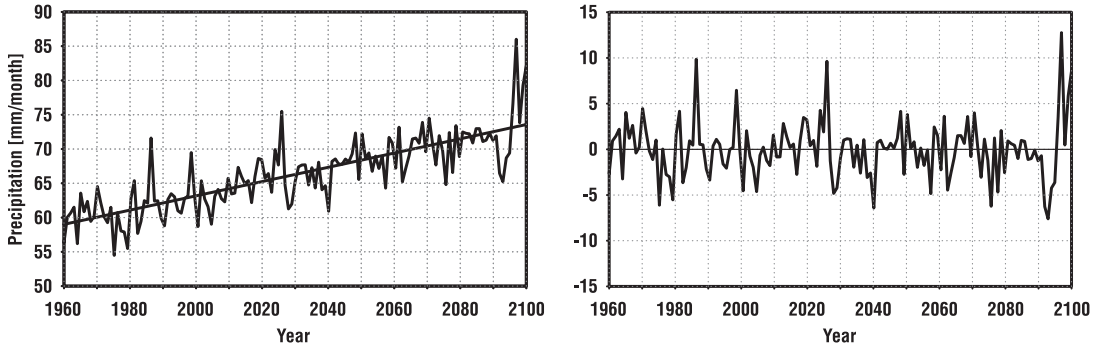


Fig. 8. Annual mean precipitation rate (mm month^{-1}) from the CCC-run from 1960–2100 (left) and its variability (right).

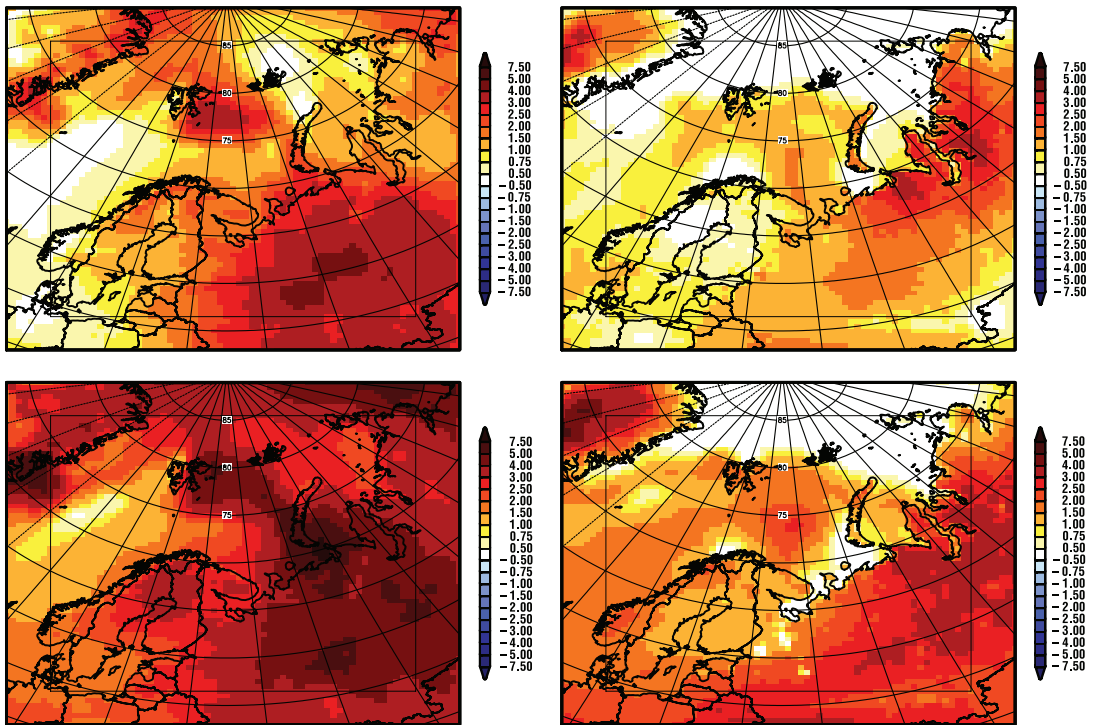


Fig. 9. Differences (time slice – control) of the mean 2-m temperatures ($^{\circ}\text{C}$) for January on the left-hand side and for July on the right-hand side for the time slice 2011–2030 above and for the time slice 2041–2060 below.

To investigate decadal changes three 20-year periods have been defined: a control period 1981–2000, and two future 20-year periods 2011–2030 and 2041–2060 (marked in Fig. 6). Only differences of the horizontal pattern of these time slices will be presented to point out where the biggest changes occur in the simulation. The differences (future decade – control) of 2-m temperature are shown in Fig. 9. A stronger warming in January than in July is evident

for both time slices. As expected, the warming is enhanced for the period 2041–2060 relative to the earlier period (2011–2030). The largest warming is located along the sea ice edge and over Russia for January 2041–2060 with temperature anomalies of more than 6°C . There exist strong differences between snow-covered and snow-free areas and between ice covered surfaces and those without ice, respectively, in surface albedo. The significantly higher amount of

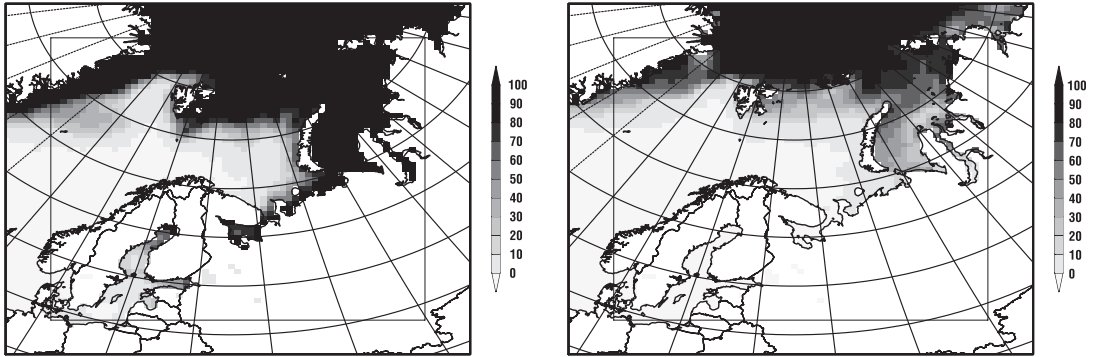


Fig. 10. Sea ice cover (%) for the mean of the time slice from 1981 until 2000 for January on the left-hand side and for July on the right-hand side.

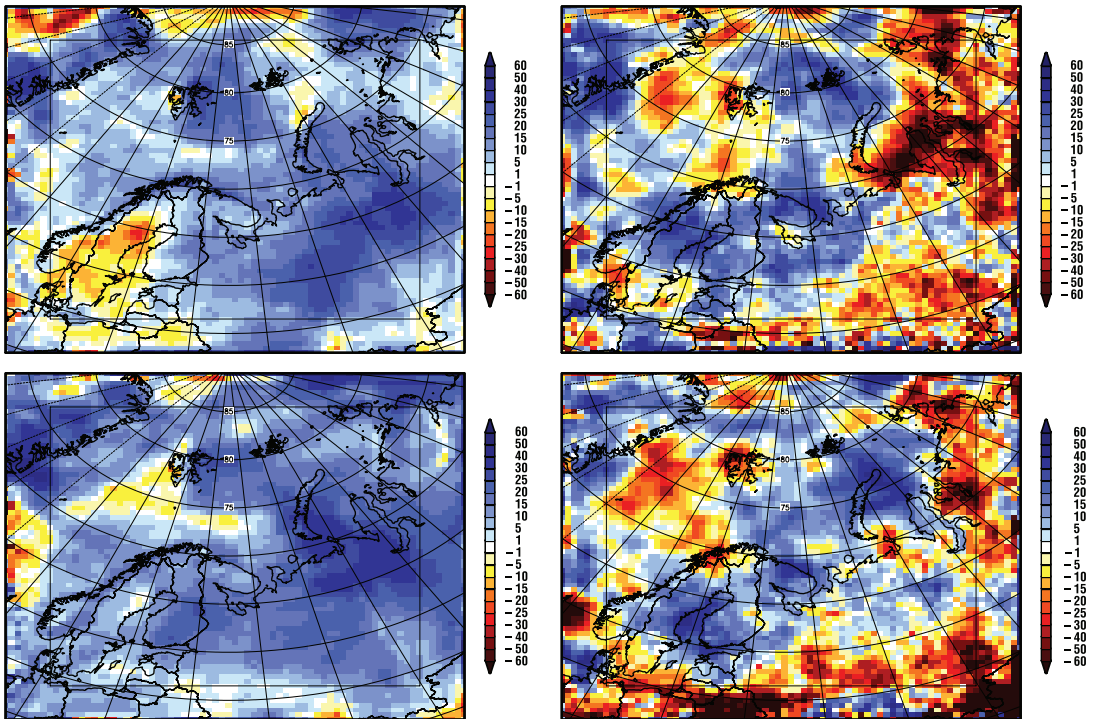


Fig. 11. Differences of the precipitation fields for January on the left-hand side and for July on the right-hand side, for the first time slice (2011–2030 – control) above and for the second time slice (2041–2060 – control) below.

solar energy absorbed on snow and ice-free areas results in the documented warming evident for January in areas south of 70°N (Fig. 9). For the other areas north of 70°N where the solar insolation is negligible the heat exchange between the sea water and the atmosphere is enhanced for ice-free areas. Therefore, the temperature change is largest along the sea ice edge and along the previously snow-covered land surfaces. The distribution of today's sea ice cover is documented

in Fig. 10 to show the location of the sea ice edge in January and July. The reduction of the sea ice cover for the two future periods takes place near the islands of Spitzbergen, Franz-Josef Land and Novaja Zeml'a for January. For July the strongest reduction is located more northwards in the northern part of the Barents Sea.

Changes in precipitation for January (left panel) and July (right panel) are illustrated in Fig. 11 and specified in Table 1. The maximum

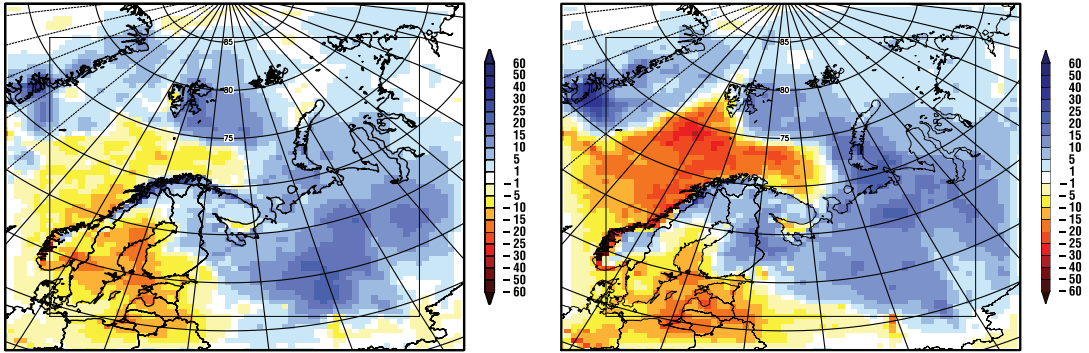


Fig. 12. Climate change signal shown as differences (time slice – control) for snow fall (mm month^{-1}) in January for the first time slice (2011–2030 – control) on the left-hand side and for the second time slice (2041–2060 – control) on the right-hand side.

mean precipitation sum for January in the control period (1981–2000) adds up to $150\text{--}200 \text{ mm month}^{-1}$ along the Norwegian coast. Mean precipitation rates occur over the Barents Sea and over Russia and amount to about $40\text{--}50 \text{ mm month}^{-1}$. In the precipitation anomaly fields for January in Fig. 11 a precipitation increase of about 5 mm month^{-1} for the first time slice (2011–2030) as mean over the simulation domain is visible. Locally the precipitation rate anomaly attains maximum values around 70 mm month^{-1} . For the later period (2041–2060) this signal is enhanced, the regional mean increase amounts to 8 mm month^{-1} . In addition, the precipitation decreases over the Baltic Sea and Scandinavia for the first 20-year period in January. The opposite signal is seen in the climate change pattern for the later 20-year period (2041–2060). The precipitation rate over the Baltic Sea and Scandinavia increases. For July the precipitation rate anomaly fields have different structures as compared with those occurring in January. A decrease of the precipitation rate over the Barents Sea is evident for both periods in contrast to an increase of precipitation over land. The increase of precipitation is slightly larger for the first 20-year period, both signals have the same sign.

Finally, changes in snow are investigated. In January, changes in snowfall rate share common features with the changes in precipitation. The snowfall rate is enhanced over land and along the sea ice edge from Novaja Zemlja, over Spitzbergen to Greenland up to 30 mm month^{-1} (Fig. 12). A decrease of snowfall occurs over Scandinavia,

the Baltic Sea and the European North Sea. This decrease is enhanced for the later period (2041–2060). Nevertheless the warming trend leads to a considerable decrease in snow cover over the Barents Sea region. Almost all of Norway, except the Norwegian coast, experiences in the control period more than 180 “snow days” a year, defined here as a day with more than 3 cm water equivalent of snow depth (Fig. 13). In contrast, in the scenario more than 180 snow days in Norway appear only at higher latitudes towards the north. The 180-snow day line moves from its current position about 300 to 500 km to the north. The longer snow-free time and the increase of the temperatures have important consequences for the vegetation in the arctic and subarctic. Rustad *et al.* (2001) showed in field experiments a temperature induced increased mineralization and plant productivity. According to Sonesson and Hoogesteger (1983) a shift of the tree lines to higher altitudes could be expected.

Table 1. Minimum, mean and maximum differences (time slice – control) of the mean precipitation (mm month^{-1}) rate for the model region of the investigated 20-year periods for January and July.

Time slice	Month	Min	Mean	Max
2011–2030 – control	January	–18.9	5.5	72.3
	July	–41.3	0.2	46.2
2041–2060 – control	January	–20.0	8.0	94.5
	July	–40.1	–0.1	43.5

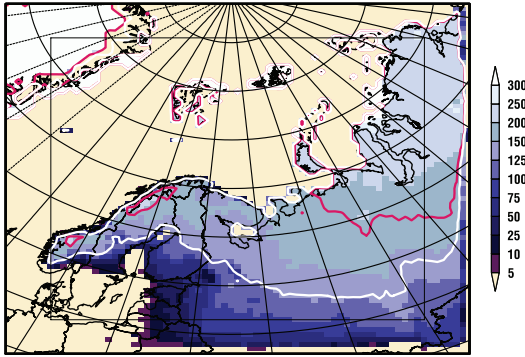


Fig. 13. Number of “snow days” over land, with a snow depth of more than 3 cm water equivalent in the scenario, for annual mean over 20 years. The area with more than 180 snow days per year is indicated with white (1981–2000) and purple (2080–2099) lines.

Conclusions

A regional climate simulation (baseline run) with REMO using 50 km horizontal resolution driven by ECMWF-Analysis/Reanalysis from 1979 until 2000 has been performed to reconstruct realistic temperature and precipitation fields for today’s climate in the Barents Sea region. Our model results have been compared to the CRU data set, which encompasses unfortunately only a few measurement stations in high latitudes. Despite some biases in the investigated regions the simulated temperature and precipitation fields seem to be realistic, but further comparisons with measured data are still desirable. Nevertheless the observed temperature increase for the Arctic is well captured by our results (ACIA, 2004: Impacts of a warming arctic, <http://amap.no/acia>).

In the CCC run the largest surface temperature changes occur during winter months due to changes of the sea ice cover. This implies that the annual cycle of the signal is varying, with a strong signal in winter and a less strong warming during summer months.

The annual mean temperature difference between the present (1970–1979) and the future Arctic climate (2070–2079) amounts to about 5.5 K and the annual mean precipitation rises about 80 mm as shown in Pfeifer and Jacob (2005). The results in this study point to the same direction despite the fact that different time slices and

just a part of the Arctic — the Barents Sea region — were considered. Additionally an increase of precipitation, which differs between January and July, was detected. The increase of snowfall rate for the first 20-year period is in agreement with the increase of precipitation, the decrease of snowfall rate is evident for the later 20-year period as expected for a slightly warmer climate. As a consequence of the warming, the biomass production and the location of tree-lines would be expected to be changed as well.

It would be useful to have more than one realization of different scenarios to constitute the range of future regional climate conditions for the Barents Sea which might be more reliable (Räisänen *et al.* 2004). The BALANCE project focused on the vulnerability of the Barents Sea region for future climate conditions with emphasis on interdisciplinary work. Therefore as a first guess just one scenario of future climate has been calculated and analysed.

Finally, it has to be stated that only the possible regional atmospheric response to global warming has been analyzed without taking into account the feedbacks of the Barents Sea as a part of the Arctic Ocean and the vegetation (Graham *et al.* 2004). Every change of the atmospheric quantities could be different if a coupled ocean/atmosphere/land/hydrology regional climate model would be used.

Additional sensitivity experiments are in preparation to study the influence of the sea surface temperature, the vegetation ratio and the forest cover separately. The BALANCE partners will provide fields of these quantities representative for the time periods under investigation.

Acknowledgements: We thank Ralf Podzun for technical support with REMO. Additionally we thank Dr. rer. nat. Susanne Pfeifer and Dr. habil. Andreas Chlond for the internal review of this paper. This work has been supported by the Fifth Framework Program of the European Commission (1998–2002) within the Program on Energy, Environment and Sustainable Development (BALANCE, EVK2-CT-2002-00169).

References

- Dethloff K., Abegg C., Rinke A., Hebestadt I. & Romanov V. 2001. Sensitivity of Arctic climate simulations to different boundary layer parameterizations in a regional climate model. *Tellus* 53A: 1–26.

- Dethloff K., Rinke A., Lehmann R., Christensen J.H., Botzet M. & Machenhauer B. 1996. A regional climate model of the Arctic atmosphere. *J. Geophys. Res.* 101: 23401–23422.
- Houghton J.T., Ding Y., Griggs D.J., Nouger M., van der Linden P.J., Dai X., Maskell K. & Johnson C.A. 2001. *Climate Change 2001. The scientific basis*, Contribution of Working Group I to the Third Assessment Report of the Governmental Panel on Climate Change, Cambridge University Press.
- Jacob D. 2001. A note to the simulation of annual and inter-annual variability of water budget over the Baltic Sea drainage basin. *Meteor. Atmos. Phys.* 77: 61–73.
- Jacob D. & Podzun R. 1997. Sensitivity studies with the regional climate model REMO. *Meteor. Atmos. Phys.* 63: 119–129.
- Jacob D., Van den Hurk B. J. J. M., Andrae U., Elgered G., Fortelius C., Graham L.P., Jackson S.D., Karstens U., Koepken C., Lindau R., Podzun R., Rockel B., Rubel F., Sass B.H., Smith R. & Yang X. 2001. A comprehensive model intercomparison study investigating the water budget during the PIDCAP period. *Meteor. Atmos. Phys.* 77: 19–44.
- Lynch A.H., Maslanik J.A. & Wu W. 2001. Mechanisms in the development of anomalous sea ice extent in the western Arctic: A case study. *J. Geophys. Res.* 106: 28097–28105.
- Lynch A.H., Chapman W.L., Walsh J.E. & Weller G. 1995. Development of a regional climate model of the western Arctic. *J. Climate* 8: 1555–1570.
- Lynch A.H., Curry J.A., Brunner R.B. & Maslanik J.A. 2004. Toward an integrated assessment of the impacts of extreme wind events on Barrow, AK. *Bull. Amer. Meteor. Soc.* 85: 209–221.
- Nakićenović N., Alcamo J., Davis G., de Vries B., Fenhann J., Gaffin S., Gregory K., Grübler A., Jung T.Y., Kram T., La Rovere E.L., Michaelis L., Mori S., Morita T., Pepper W., Pitcher H., Price L., Raihi K., Roehrl A., Rogner H.-H., Sankovski A., Schlesinger M., Shukla P., Smith S., Swart R., van Rooijen S., Victor N. & Dadi Z., 2000: *IPCC special report on emissions scenarios*, Cambridge University Press, Cambridge, United Kingdom and New York, NY, USA.
- New M., Lister D., Hulme M. & Makin I. 2002. A high resolution data set of surface climate over global land areas. *Clim. Res.* 21: 1–25.
- Pfeifer S. & Jacob D. 2005. Changes of the Arctic climate under the SRES B2 scenario conditions simulated with the regional climate model REMO. *Meteorologische Zeitschrift* 16: 711–719.
- Przybylak R. 2002. Variability of air temperature and atmospheric precipitation in the Arctic. *Atmospheric and Oceanographic Sciences Library* 25: 1–330.
- Räisänen J., Hansson U., Ullerstig A., Döscher R., Graham L.-P., Jones C., Meier H.E.M., Samuelsson P. & Willen U. 2004. European climate in the late twenty-first century: regional simulations with two driving global models and two forcing scenarios. *Clim. Dyn.* 22: 13–31.
- Raschke E., Karstens U., Nolte-Holube R., Brandt R., Isemer H.-J., Hoffmann D., Lobmeyer M., Rockel B. & Stuhlmann R. 1998. The Baltic Sea Experiment BALTEX: A brief overview and some selected results of the authors. *Surv. Geophys.* 19: 1–22.
- Raschke E., Meywerk J., Warrach K., Andrae U., Bergstroem S., Beyrich F., Bosveld F., Bumke K., Fortelius C., Graham L.P., Gryning S.-E., Halldin S., Hasse L., Heikinheimo M., Isemer H.-J., Jacob D., Jauja I., Karlsson K.-G., Keevallik S., Koistinen J., van Lammeren A., Lass U., Launiainen J., Lehmann A., Liljebladh B., Lobmeyer B., Matthäus W., Mengelkamp T., Michelson D.B., Napiorkowski J., Omstedt A., Piechura J., Rockel B., Rubel F., Ruprecht E., Smedman A.-S. & Stigebrandt A. 2001. BALTEX (Baltic Sea Experiment): A European contribution to investigate the energy and water cycle over a large drainage basin. *Bull. Amer. Meteor. Soc.* 82: 2389–2413.
- Rinke A., Dethloff K., Cassano J., Christensen J.H., Curry J.A., Du P., Girard E., Haugen J.-E., Jacob D., Jones C., Koltzow M., Laprise R., Lynch A.H., Pfeifer S., Serreze M.C., Shaw M.J., Tjernström M., Wyser K. & Zagar M. 2006. Evaluation of an ensemble of Arctic regional climate models: spatial patterns and height profiles. *Clim. Dyn.* 26, doi:10.1007/s00382-005-0095-3.
- Roeckner E., Bengtsson L., Feichter J., Lelieveld J. & Rohde H. 1999. Transient climate change simulations with a coupled atmosphere–ocean GCM including the tropospheric sulfur cycle. *J. Climate* 12: 3004–3032.
- Rustad L.E., Campbell J.L., Marion G.M., Norby R.J., Mitchell M.J., Hartley A.E., Cornelissen J.H.C., Gurevitch J. & GCTE-NEWS 2001. A meta-analysis of the response of soil respiration, net nitrogen mineralization, and aboveground plant growth to experimental ecosystem warming. *Oecologia* 126: 543–562.
- Semmler T. 2002. *Der Wasser- und Energiehaushalt der arktischen Atmosphäre*. Ph.D. thesis, Max-Planck-Institut für Meteorologie Hamburg.
- Sonesson M. & Hoogesteger J. 1983. Recent tree line dynamic (*Betula pubescens* Ehrh. ssp. *tortuosa* (Ledeb.) Nyman) in northern Sweden. *Nordica* 47: 47–54.
- Tjernström M., Zagar M., Svensson G., Cassano J.J., Pfeifer S., Rinke A., Wyser K., Dethloff K., Jones C. & Semmler T. 2005. Modeling the Arctic boundary layer: an evaluation of six ARCMIP regional-scale models with data from the SHEBA project. *Bound.-Layer Meteor.* 117: 337–381.